in combination with tamoxifen versus tamoxifen alone for adjuvant treatment of postmenopausal woman with early breast cancer: first results of the ATAC randomised trials. Lancet 359:2131–2139

Buzdar A, Howell A, Cuzick J, Wale C, Distler W, Hoctin-Boes G, Houghton J, Locker GY, Nabhholtz JM, ATAC Trialists' Group (2006) Comprehensive side-effect profile of anastrozole and tamoxifen as adjuvant treatment for early-stage breast cancer: long-term safety analysis of the ATAC trial. Lancet Oncol 7:633–643

Crew KD, Greenlee H, Capodice J, Raptis G, Brafman L, Fuentes D, Sierra A, Hershman DL (2007) Prevalence of joint symptoms in postmenopausal women taking aromotase inhibitors for early-stage breast cancer. J Clin Oncol 25:3877–3883

Donnellan PP, Douglas SL, Cameron DA, Leonard RC (2001) Aromatase inhibitors and arthralgia. J Clin Oncol 19:2767

Howell A, Cuzick J, Baum M, Buzdar A, Dowsett M, Forbes JF, Hoctin-Boes G, Houghton J, Locker GY, Tobias JS, ATAC Trialist's Group (2005) Results of the ATAC trial after completion of 5 years' adjuvant treatment for breast cancer. Lancet 365:60–62

Ito M, Lang TF, Jergas M, Ohki M, Takada M, Nakamura T, Hayashi K, Genanat HK (1997) Spinal trabecular bone loss and fracture in American and Japanese women. Calcif Tissue Int 61:123–128

Ohsako T, Inoue K, Nagamoto N, Yoshida Y, Nakahara O, Sakamoto N (2006) Joint symptoms: a practical problem of anastrozole. Breast Cancer 13:284–288

Ross PD, Fujiwara S, Huang C, Davis JW, Epstein RS, Wasnich RD, Kodama K, Melton LJ III (1995) Vertebral fracture prevalence in women in Hiroshima compared to Caucasians or Japanese in the US. Int J Epidemiol 24:1171–1177

Shimizu H, Ross RK, Bernstein L, Pike MC, Henderson BE (1990) Serum oestrogen levels in postmenopausal women: comparison of American whites and Japanese. Br J Cancer 62:451–453

Yoneda K, Tanji Y, Okishiro M, Taguchi T, Tamaki Y, Noguchi S (2006) Influence of adjuvant anastrozole on bone mineral density in Japanese postmenopausal breast cancer patients: is there a racial difference? Ann Oncol 17:1175–1176

Available online at www.sciencedirect.com
ScienceDirect
Cancer Letters 262 (2008) 248–256
CANCER Letters
www.elsevier.com/locate/canlet

Connexin26 expression is associated with aggressive phenotype in human papillary and follicular thyroid cancers

Yasuto Naoi, Yasuo Miyoshi, Tetsuya Taguchi, Seung Jin Kim, Takashi Arai, Naomi Maruyama, Yasuhiro Tamaki, Shinzaburo Noguchi *

Department of Breast and Endocrine Surgery, Osaka University Graduate School of Medicine, 2-2 Yamadaoka, Suita-shi, Osaka 567-0871, Japan

Received 22 August 2007; received in revised form 30 November 2007; accepted 3 December 2007

Abstract

Connexin26 (Cx26), a component of GAP junctions and until recently believed to be a tumor suppressor gene, has been shown to play an important role in lymphatic invasion as well as lymph node and distant metastases in squamous lung cancer and breast cancer. In the study presented here, we investigated Cx26 expression in human papillary thyroid cancer (PTC) and follicular thyroid cancer (FTC) and its relationship with various clinicopathological parameters. Of 69 PTCs, 33 were positive for Cx26 (47.8%), as were five of 11 FTCs (45.5%), all follicular thyroid adenomas ($n = 22$) and normal thyroid tissues ($n = 20$) were negative for Cx26. A statistically significant association was observed between Cx26 expression and large tumor size ($p = 0.028$ for PTC) and lymph node metastases ($p = 0.053$ (marginally significant) for PTC and $p = 0.035$ for FTC). Presence of intra-glandular dissemination of tumor cells was significantly ($p = 0.048$) more frequent in Cx26-positive (30.3%) than Cx26-negative PTCs (11.1%). Lymphatic vessel invasion was more frequent in Cx26-positive PTCs (6.1%) than in Cx26-negative PTCs (0%) though the difference was not statistically significant. These results suggest that Cx26 may be implicated in the pathogenesis of PTC and FTC and is associated with the biologically aggressive phenotypes of these tumors.

Keywords: Connexin26; Thyroid cancer; D2-40; CD34

1. Introduction

Gap junctions form channels between adjacent cells, which allow the exchange of ions, nucleotides, metabolites and other small molecules (<1 kDa) including second messengers such as Ca^{2+}, cAMP, and IP3 [1–3]. Gap junctional intercellular communication (GJIC) plays an important role in a variety of cellular processes including homeostasis, morphogenesis, cell differentiation, and growth control

Abbreviations: Cx, connexin; PTC, thyroid papillary carcinoma; FTC, thyroid follicular carcinoma; FTA, thyroid follicular adenoma; GJIC, gap junction intercellular communication.

* Corresponding author. Tel.: +81 6 6879 3772; fax: +81 6 6879 3779.
E-mail address: noguchi@onsurg.med.osaka-u.ac.jp (S. Noguchi).

0304-3835/$ - see front matter © 2007 Elsevier Ireland Ltd. All rights reserved.
doi:10.1016/j.canlet.2007.12.008

[4]. Gap junction channels are composed of two hemi-channels (connexons) and each connexon consists of six connexins. Gap junctions may be composed of different Cx isotypes (heterotypic) or of more than one Cx isotype (heteromeric) [1]. To date, 20 members of the connexin transmembrane protein family have been identified [5].

It has been shown that, loss or reduced function of GJIC is generally implicated in the progression of a variety of tumors, and is usually induced by down-regulation of connexins. Reduced expression of Cx32 in human gastric cancer [6], Cx43 in human prostatic adenocarcinoma cells [7] and human brain glioma cells [8], Cx32 and Cx43 in human lung cancer [9], and Cx43 in human breast cancer [10] have been reported. In addition, restoration of function in these connexins has been shown to result in the retardation of cell growth and induction of more normal phenotypes [11,12]. Thus, connexins are generally considered to be tumor suppressor genes [13].

Cx26 is a member of the connexin family and was initially isolated as a gene with down-regulated expression in breast cancer cell lines as compared with normal human breast epithelial cell lines [14]. Furthermore, transfection of Cx26 into various tumor cell lines including breast cancer cell lines has been shown to confer growth suppression [15–17]. Analogous to other connexins, Cx26 has thus also been considered to serve as a tumor suppressor gene. However, recent studies have disclosed a unique feature of Cx26 in tumor progression. Ito et al. [18] found that abnormally augmented expression of connexin26 is responsible for the enhanced spontaneous metastasis of mouse BL6 melanoma cells, and that the exogenous expression of a dominant negative form of Cx26 results in an increase in the spontaneous metastases of BL6. They also suggested that formation of heterologous gap junctions between Cx26 and Cx43, which are expressed in melanoma cells and vascular endothelial cells, respectively, may facilitate the invasion of tumor cells into the blood vessels. They based their suggestion on the observation that melanoma cells could transfer dye into vascular endothelial cells.

Very recently, Ito et al. also reported the up-regulation of Cx26 in human lung squamous cell cancer as well as its association with poor prognosis [19] and suggested that Cx26 may play an important role in the acquisition of malignant phenotypes. Furthermore, we were able to show that Cx26 expression is associated with lymphatic vessel invasion, large tumor size, high histological grade, and poor prognosis of human breast cancers, indicating that Cx26 seems to enhance metastasis, probably through the promotion of lymphatic vessel invasion [20].

Putting all these observations together leads to the speculation that Cx26, unlike other connexins, may be implicated in the acquisition of malignant phenotypes such as tumor invasion and metastases and that the association between Cx26 expression and malignant phenotypes may also apply to other human cancers. Since no studies of the expression of Cx26 expression in human thyroid cancers have been reported yet, we investigated, in the study presented here, the relationship between Cx26 expression and various clinicopathological parameters including lymph node metastases, lymphatic invasion, and blood vessel invasion in papillary thyroid cancer (PTC) and follicular thyroid cancer (FTC).

2. Materials and methods

2.1. Patients and tumor tissues

Surgical specimens obtained from 102 patients, who underwent hemithyroidectomy or total thyroidectomy due to PTC ($n = 69$), FTC ($n = 11$) or follicular thyroid adenoma (FTA) ($n = 22$) at Osaka University Hospital, were fixed in 10% buffered formalin and embedded in paraffin. Fresh tumor tissues and normal thyroid tissues, obtained from three PTCs, three FTAs and three normal thyroid tissues adjacent to PTC, were snap frozen in liquid nitrogen and kept at −80 °C until used for Western blotting. This study was approved by the institutional review board of Osaka University Graduate School of Medicine.

2.2. Immunohistochemistry

Paraffin sections (4 μm) of tumor tissues were subjected to immunohistochemical staining of Cx26 protein with the avidin–biotin-peroxidase method. In brief, endogenous peroxidases were quenched by incubating the sections for 20 min in 3% H_2O_2. Antigen retrieval was performed by heating the samples in 10 mmol/L citrate buffer (pH 6.0) at 95 °C for 40 min. After treatment with Block Ace (Dainippon Sumitomo Pharmaceutical, Osaka, Japan) for 30 min at room temperature, the sections were incubated at 4 °C overnight with a mouse monoclonal anti-Cx26 antibody (Catalog No.13-8100, working dilution 1:500; purchased from Zymed Laboratories Inc., South San Francisco, CA, USA). The avidin–biotin-peroxidase complex system (Vectastain® Elite ABC kit; Vector Laboratories Inc., Burlingame, CA, USA) was used for color development. The entire tumor lesion was observed with special attention to the periphery of tumors since tumor cells in the periphery of other tumors are reportedly more likely to be Cx26-positive

than those in the center [19]. For each tumor, 1000 tumor cells were counted and, when more than 10% were clearly positive for Cx26 staining, the tumor was considered to be Cx26-positive.

2.3. Lymph and blood vessel density

After immunohistochemical staining of lymphatic vessels by anti-D2-40 and of blood vessels by anti-CD34 antibodies [20], vessel density in each case was determined by counting all immunostained vessels at a magnification of 200× from five areas, and the mean was used as the blood or lymphatic vessel density of the case. Since Yasuoka et al. reported that lymphatic vessel density differs in the intratumoral and peritumoral areas in human thyroid tumors [21], blood vessel density or lymph vessel density in the intratumoral and the peritumoral areas was analyzed separately.

2.4. Immunoabsorption test

Antibody blocking experiments were performed to confirm antibody specificity. Cx26 antibody blocking peptide was purchased from Alpha Diagnostic International (San Antonio, TX, USA). Ten micrograms control peptide per 1 μg of this antibody was used and incubated at 37 °C for 1 h and centrifugal separation was conducted at 7000 rpm for 10 min. This was followed by immunohistochemistry performed according to the protocol described above.

2.5. Western blotting

Western blotting was also performed to confirm antibody specificity. After surgery, thyroid tissues were rapidly frozen and stored at −80 °C until use. In preparation for SDS–polyacrylamide gel electrophoresis (SDS–PAGE), tissue was homogenized in Tris buffer. Homogenates were sonicated, and total protein was determined. Nine lanes were prepared on the gel. Lanes 1–3 were for thyroid papillary cancer tumors which were immunohistochemically positive for Cx26, lanes 4–6 were for thyroid adenomas and lanes 7–9 were for normal thyroid tissues adjacent to thyroid cancers. Proteins were resolved by SDS–PAGE on 5–20% gel (SuperSep TM HG; Wako, Osaka, Japan), 20 μg per lane, and samples not boiled prior to loading were transblotted to 0.2 mm nitrocellulose in transfer buffer, pH 8.3. Immunoblots were blocked for 2–3 h in 4% block ace (Yukijirushi, Osaka, Japan) and incubated with anti-Cx26 antibodies (1:500 dilution) overnight at 4 °C in Can Get Signal Solution 1 (Taiho Pharmaceutical, Osaka, Japan). Membranes were washed in TBS-T and then incubated for 1 h at room temperature with a secondary antibody (anti-mouse horseradish peroxidase-conjugated IgG at 1:3000 dilution) in Can Get Signal Solution 2 (Taiho Pharmaceutical). Membranes were again washed and incubated for 5 min with the ECL Plus Western Blotting Detection System (GE Healthcare UK Ltd., Buckinghamshire, UK) for detection of immunoreactive protein.

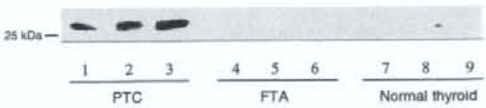

Fig. 2. Western blot analysis of Cx26. Lanes 1–3, papillary thyroid cancers immunohistochemically positive for Cx26. Lanes 4–6, follicular thyroid adenomas. Lanes 7–9, normal thyroid tissues.

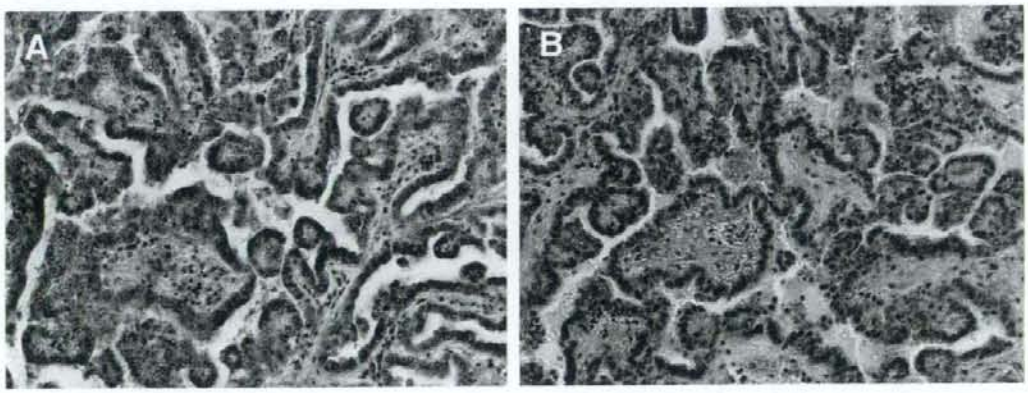

Fig. 1. Immunoabsorption study. Paraffin sections from papillary thyroid cancer were incubated with anti-Cx26 antibody in the absence (A) or presence (B) of pretreatment with excess amount of the same peptide used to generate this antibody (200×).

2.6. Statistics

Chi-square test or Mann–Whitney's *U*-test was used for analysis of the relationship between Cx26 expression and clinicopathological parameters of thyroid tumors. Statistical significance was defined as $p < 0.05$.

3. Results

3.1. Specificity of immunohistochemical examination of Cx26

In order to prove the specificity of immunostaining of Cx26, we carried out an immunoabsorption study, i.e., paraffin sections from Cx26-positive PTCs were incubated with anti-Cx26 antibody in the absence (Fig. 1A) or presence (Fig. 1B) of pretreatment with an excess amount of the same peptide which had been used to generate this antibody. The positive signal in tumor cells seen in Fig. 1A (without pretreatment) almost completely disappeared as seen in Fig. 1B (with pretreatment), indicating that immunohistochemical examination using this antibody is specific to Cx26. Western blotting of Cx26 using fresh tissue samples from PTCs, FTAs, and normal thyroid tissues was also performed. Cx26 expression was observed only in PTCs but not in FTAs or normal thyroid tissues (Fig. 2), so that these results were consistent with those obtained by immunohistochemistry.

3.2. Immunohistochemical examination of Cx26 expression in PTC, FTC, and FTA

Of the 69 PTCs, 33 were positive for Cx26 (47.8%), and of the 11 FTCs, five were positive for Cx26 (45.5%). All FTAs ($n = 22$) and normal thyroid tissues ($n = 20$) were negative for Cx26. Representative results of immunohisto-

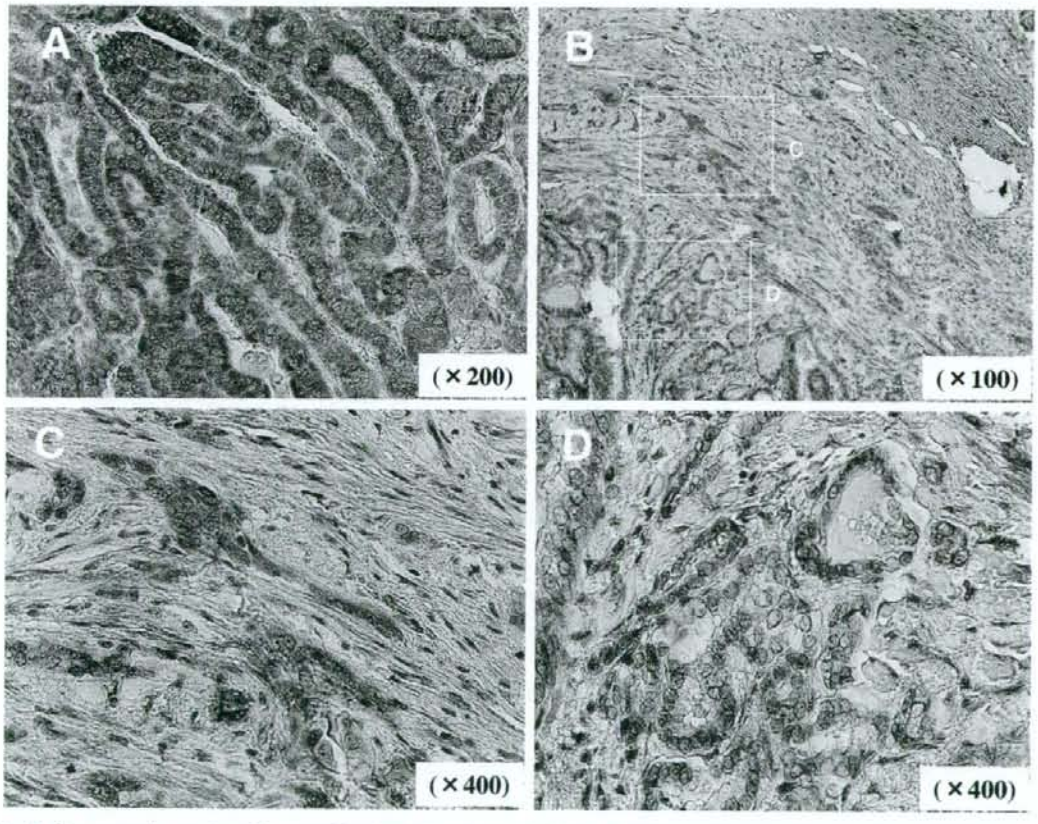

Fig. 3. Representative results of immunohistochemical staining of Cx26. (A) Papillary thyroid cancer strongly positive for Cx26 immunostaining (200×). (B) When a small percentage of tumor cells (about 10% in this tumor) was positive for Cx26 immunostaining, positive tumor cells were mostly observed in the periphery (100×). (C) Cx26-positive tumor cells in the periphery and (D) Cx26-negative tumor cells in the center of a tumor (400×).

chemical examination of Cx26 expression in thyroid cancer tissues are shown in Fig. 3. Fig. 3A shows a PTC positive for Cx26 immunostaining with cytoplasmic staining observed in almost all tumor cells. Fig. 3B shows a PTC with about 10% of tumor cells positive for Cx26 staining. In such a weakly positive tumor, Cx26-positive tumor cells were mostly observed in the periphery (Fig. 3C), but not in the center (Fig. 3D).

3.3. Relationship between Cx26 expression and clinicopathological features of thyroid cancers

A statistically significant association was observed between Cx26 expression and large tumor size ($p = 0.028$ for PTC) and lymph node metastases ($p = 0.053$ (marginally significant) for PTC and $p = 0.035$ for FTC) (Tables 1 and 2). Presence of intra-glandular dissemination of tumor cells was significantly ($p = 0.048$) more frequent in Cx26-positive (30.3%) than in Cx26-negative PTCs (11.1%). There was no significant association between Cx26 expression and histological type of PTCs (Table 1) or invasion type of FTCs (Table 2).

Tumor cell invasion into the lymphatic vessels and blood vessels was immunohistochemically evaluated by using anti-D2-40 and anti-CD34 antibodies to visualize the lymphatic vessels and blood vessels, respectively. Representative results of lymphatic vessel invasion and blood vessel invasion are shown in Fig. 4, where Cx26-positive tumor cells are seen in both lymphatic and blood vessels. Lymphatic vessel invasion was more frequent in Cx26-positive PTCs (6.1%) than in Cx26-negative PTCs (0%) and blood vessel invasion was more frequent in Cx26-positive PTCs (12.1%) than in Cx26-negative PTCs (5.6%) though neither was statistically significant (Table 1).

Table 1
Relationship between Cx26 expression and clinicopathological parameters in thyroid papillary cancers

	Cx26 expression		p
	Negative	Positive	
Tumor size			
T1 (≦2 cm)	23	13	0.028
T2 (>2, ≦4cm)	9	11	
T3 (>4 cm)	4	8	
T4 (Invasion)	0	1	
Lymph node metastasis			
Positive	18	24	0.053
Negative	18	9	
Lymphatic vessel invasion			
Positive	0	2	0.145
Negative	36	31	
Blood vessel invasion			
Positive	2	4	0.334
Negative	34	29	
Dissemination			
Positive	4	10	
Negative	32	23	0.048
Histological type			
Classical type	28	31	0.203
Follicular variant	6	1	
Encapsulated variant	1	1	
Oxyphilic cell variant	1	0	

Table 2
Relationship between Cx26 expression and clinicopathological parameters in thyroid follicular cancers

	Cx26 expression		p
	Negative	Positive	
Tumor size			
T1 (≦2 cm)	2	2	0.632
T2 (>2, ≦4 cm)	1	0	
T3 (>4 cm)	3	3	
T4 (Invasion)	0	0	
Lymph node metastasis			
Positive	1	4	0.035
Negative	5	1	
Lymphatic vessel invasion			
Positive	0	0	...
Negative	6	5	
Blood vessel invasion			
Positive	1	0	0.338
Negative	5	5	
Invasion type			
Minimally invasive	4	5	0.154
Widely invasive	2	0	

3.4. Relationship between Cx26 expression and lymphatic or blood vessel density

A statistically significant ($p = 0.023$) association was observed between peritumoral, but not intratumoral, lymphatic vessel density and lymph node metastasis in PTCs (Table 3). There was a non-significant ($p = 0.099$) tendency for peritumoral lymph vessel density to be associated with Cx26 expression in PTCs (Table 3).

3.5. Comparison of Cx26 expression in primary tumor and lymph node metastases

In 22 PTCs with lymph node metastases, Cx26 expression was compared in primary tumors and lymph node metastases, but no significant difference was observed (Fig. 5).

4. Discussion

We were able to demonstrate immunohistochemically that Cx26 was positive in 47.8% of PTCs and

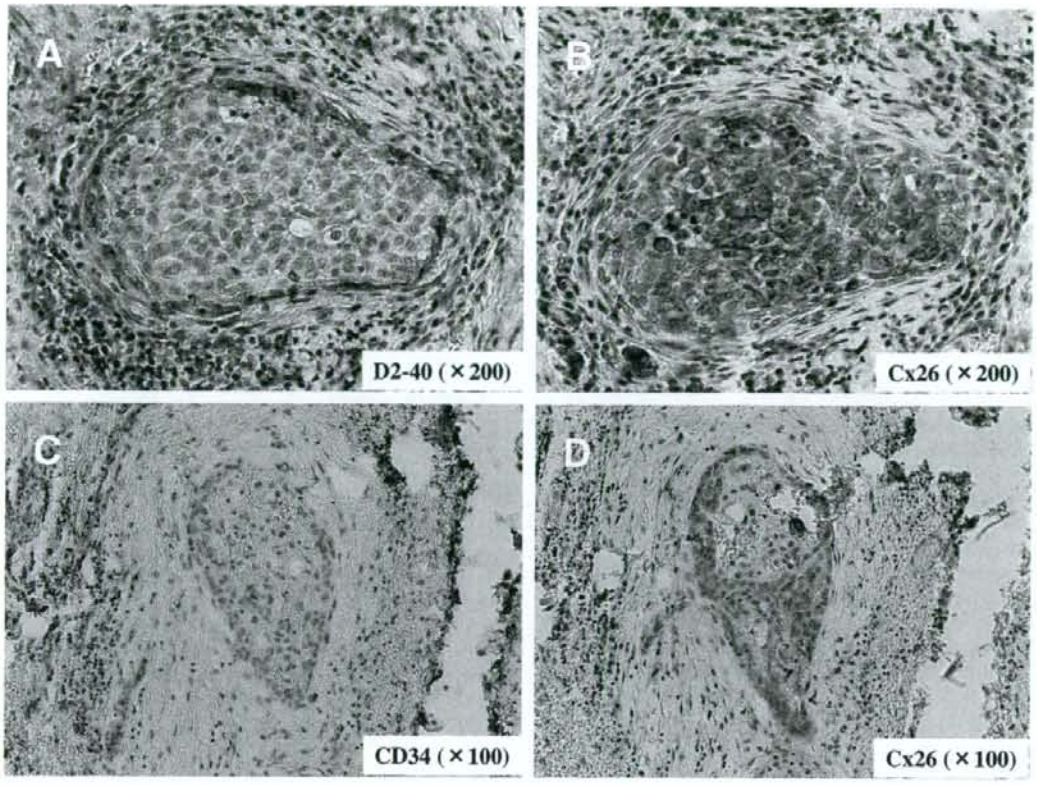

Fig. 4. Representative findings of lymphatic vessel invasion and blood vessel invasion. (A) Lymphatic vessel invasion detected by immunostaining with an anti-D2-40 antibody (200×). (B) In the section next to (A), Cx26-positive tumor cells were observed in the lymphatic vessel (200×). (C) Blood vessel invasion detected by immunostaining with an anti-CD34 antibody (100×). (D) In the section next to (C), Cx26-positive tumor cells were observed in the blood vessel (100×).

Table 3
Relationship between lymph node metastasis and vessel density

	Lymph node metastasis			Cx26 expression		
	Negative	Positive	*p*-Value	Negative	Positive	*p*-Value
Blood vessel density						
Intratumoral	223 ± 15.6[a]	17.6 ± 11.9	0.257	21.2 ± 15.8	17.6 ± 10.7	0.371
Peritumoral	26 ± 2.2	3.7 ± 4.6	0.981	3.9 ± 4.6	2.6 ± 2.9	0.232
Lymphatic vessel density						
Intratumoral	09 ± 2.1	1.9 ± 4.3	0.329	1.7 ± 3.7	1.2 ± 3.6	0.509
Peritumoral	4.8 ± 5.6	8.2 ± 7.7	0.023	5.6 ± 6.6	8.1 ± 7.4	0.099

Mann–Whitney *U*-test was used to examine the relationship between lymph node metastasis and the density of each vessel.
[a] Mean ± SD/field.

45.5% of FTCs but not in FTAs or normal thyroid tissues. These findings seem to be incompatible with the generally accepted thesis that Cx26 is a tumor suppressor gene, but rather to indicate a possible involvement of Cx26 in the pathogenesis of thyroid cancers. Furthermore, we could show in this study a significant association between Cx26 expression and large tumor size, lymph node metastasis and intra-

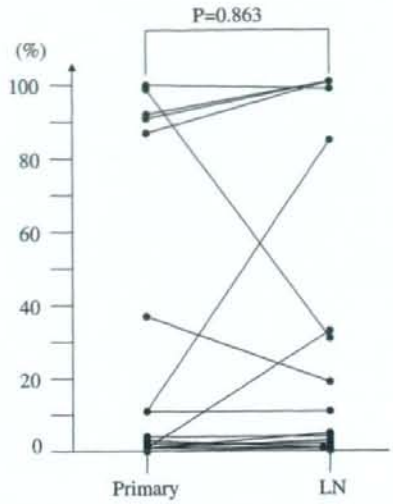

Fig. 5. Comparison of Cx26 expression in primary papillary thyroid cancers and matched lymph node metastases. Paired *t*-test was used to examine the association.

glandular dissemination in PTC, suggesting that Cx26 expression is associated with a biologically aggressive phenotype. These observations are consistent with recent reports that Cx26-positive squamous cell lung cancers are associated with a high recurrence rate [19], that Cx26-positive BL6 mouse melanoma cells increase metastatic properties [18], and that Cx26-positive breast cancers are associated with lymphatic vessel invasion, large tumor size, high histological grade, and poor prognosis [20]. We therefore speculate that the association of Cx26 expression with biologically aggressive phenotype is not a rare phenomenon seen in a few types of tumors but rather a ubiquitous occurrence in a variety of tumors. Although connexins have been characterized as a tumor suppressor gene in several types of cancers [7–9,11,12,22–26], our observations reported here seem to indicate the need for a re-evaluation of the role of Cx26 in the pathogenesis of these tumors.

Staining of Cx26 was mostly observed in the cytoplasm of tumor cells (Fig. 1A), as previously reported for colorectal cancer [3], human breast cancer [20] and squamous lung cancer [19]. Cytoplasmic expression of Cx26 may constitute indirect evidence of a lack of functional gap junction channels between cancer cells which may thus facilitate the local invasion of tumor cells. Interestingly, we were able to show in a previous study on breast cancer that lymphatic vessel invasion was significantly ($p = 0.001$) more frequent in Cx26-positive tumors (39.7%) than in Cx26-negative tumors (14.9%). In this study on thyroid cancer, we could show a non-significant tendency for Cx26 expression to be associated with lymphatic vessel invasion as well as a significant association between Cx26 expression and intra-glandular dissemination or lymph node metastases. Since intra-glandular dissemination of tumor cells is considered to be a sign of lymphatic vessel invasion, our findings seem to suggest that, like Cx26-positive breast cancer cells, Cx26-positive thyroid cancer cells also have a propensity to invade the lymphatic vessels, resulting in the development of lymph node metastases. It is speculated that such a propensity stems from the formation of a heterologous gap junction between Cx26-expressing tumor cells and Cx43-expressing vascular endothelial cells [27,28], leading to the invasion of tumor cells into the lymphatic vessels.

We previously reported [20] that Cx26-positive tumor cells in breast cancer are mostly localized in the periphery (invasion front) of a tumor when Cx26 is weakly positive. Such a peripheral localization of Cx26-positive tumor cells was also observed in PTC. In addition, a statistically significant association was observed between peritumoral lymph vessel density and lymph node metastases in PTC. Putting these finding together makes it tempting to speculate that Cx26-positive tumor cells localizing in the invasion front, even if their number is small, seem to have a good opportunity to invade the adjacent lymphatic vessels. Interestingly, there was also a tendency for Cx26 positivity to be associated with peritumoral lymphatic vessel density. Cx26-positive thyroid cancer cells appear to be very likely to invade the lymphatic vessels. Their intense invasiveness is due to lack of GJIC, formation of heterologous gap junctions with lymphatic vessels, and easy accessibility of lymphatic vessels in the periphery of a tumor.

Koda et al. reported that Cx26 expression is higher in lymph node metastases than in primary tumors in breast cancers, suggesting that Cx26-positive tumor cells are more likely than Cx26-negative tumor cells to invade the lymphatic vessels and metastasize to the lymph nodes [29]. We therefore compared Cx26 expression in primary tumors and lymph node metastases in PTC, but were unable to detect an increased expression of Cx26 in lymph node metastases. Although the reason for this discrepancy is currently unknown, the role of Cx26 in the development of

lymph node metastases may be much more important in breast cancer than in thyroid cancer.

In conclusion, our results suggest that Cx26 may be involved in pathogenesis and is associated with biologically aggressive phenotypes such as large tumor size and lymph node metastases in PTC and FTC. Cx26 seems to function not as a tumor suppressor gene but as an oncogene in these tumors. The limitation of the present study is such a small number of analyzed tumors, especially, FTCs, that a definitive conclusion can not be drawn. Thus, our preliminary observation needs to be validated in a future study including a larger number of tumors with various histological types.

Acknowledgement

Grant support: Grant-in-Aid for Scientific Research on Priority Areas from the Ministry of Education, Culture, Sports, Science and Technology of Japan.

References

[1] N.M. Kumar, N.B. Gilula, The gap junction communication channel, Cell 84 (1996) 381–388.
[2] R. Bruzzone, T.W. White, D.L. Paul, Connections with connexins: the molecular basis of direct intercellular signaling, Eur. J. Biochem. 238 (1996) 1–27.
[3] L. Kanczuga-Koda, S. Sulkowski, M. Koda, E. Skrzydlewska, M. Sulkowska, Connexin26 correlates with Bcl-xL and Bax proteins expression in colorectal cancer, W. J. Gastroenterol. 10 (2005) 1544–1548.
[4] V.A. Krutovskikh, C. Piccoli, H. Yamasaki, Gap junction intercellular communication propagates cell death in cancerous cells, Oncogene 21 (2002) 1989–1999.
[5] K. Willecke, J. Eiberger, J. Degen, D. Eckardt, A. Romualdi, M. Guldenagel, U. Deutsch, G. Sohl, Structural and functional diversity of connexin genes in the mouse and human genome, Biol. Chem. 383 (2002) 725–737.
[6] A. Nagahara, S. Watanabe, H. Miwa, K. Endo, M. Hirose, N. Sato, Reduction of gap junction protein connexin32 in rat atrophic gastric mucosa as an early event in carcinogenesis, J. Gastroenterol. 31 (1996) 491–497.
[7] H. Tsai, J. Werber, M.O. Davia, M. Edelman, K.E. Tanaka, A. Melman, G.J. Christ, J. Geliebter, Reduced connexin43 expression in high grade, human prostatic adenocarcinoma cells, Biochem. Biophys. Res. Commun. 227 (1996) 64–69.
[8] R.P. Huang, M.Z. Hossain, A. Sehgal, A.L. Boynton, Reduced connexin43 expression in high-grade human brain glioma cells, J. Surg. Oncol. 70 (1999) 21–24.
[9] Y. Jinn, M. Ichioka, F. Marumo, Expression of connexin32 and connexin43 gap junction proteins and E-cadherin in human lung cancer, Cancer Lett. 127 (1998) 161–169.
[10] D.W. Laird, P. Fistouris, G. Batist, L. Alpert, H.T. Huynh, G.D. Carystinos, M.A. Alaoui-Jamali, Deficiency of connexin43 gap junctions is an independent marker for breast tumors, Cancer Res. 59 (1999) 4104–4110.
[11] B. Eghbali, J.A. Kessler, L.M. Reid, C. Roy, D.C. Spray, Involvement of gap junctions in tumorigenesis: transfection of tumor cells with connexin32 cDNA retards growth in vivo, Proc. Natl. Acad. Sci. USA 88 (1991) 10701–10705.
[12] R.P. Huang, Y. Fan, M.Z. Hossain, A. Peng, Z.L. Zeng, A.L. Boynton, Reversion of the neoplastic phenotype of human glioblastoma cells by connexin43 (cx43), Cancer Res. 58 (1998) 5089–5096.
[13] J.E. Trosko, R.J. Ruch, Cell–cell communication in carcinogenesis , Front. Biosci. 3 (1998) d208–d236.
[14] S.W. Lee, C. Tomasetto, D. Paul, K. Keyomarsi, R. Sager, Transcriptional downregulation of gap-junction proteins blocks junctional communication in human mammary tumor cell lines, J. Cell Biol. 118 (1992) 1213–1221.
[15] P. Hellmann, R. Grummer, K. Schirrmacher, M. Rook, O. Traub, E. Winterhager, Transfection with different connexin genes alters growth and differentiation of human choriocarcinoma cells, Exp. Cell Res. 246 (1999) 480–490.
[16] H.J. Lee, I.K. Lee, K.H. Seul, S.K. Rhee, Growth inhibition by connexin26 expression in cultured rodent tumor cells, Mol. Cells 14 (2002) 136–142.
[17] M. Momiyama, Y. Omori, Y. Ishizaki, Y. Nishikawa, T. Tokairin, J. Ogawa, K. Enomoto, Connexin26-mediated gap junctional communication reverses the malignant phenotype of MCF-7 breast cancer cells, Cancer Sci. 94 (2003) 501–507.
[18] A. Ito, F. Katoh, T.R. Kataoka, M. Okada, N. Tsubota, H. Asada, K. Yoshikawa, S. Maeda, Y. Kitamura, H. Yamasaki, H. Nojima, A role for heterologous gap junctions between melanoma and endothelial cells in metastasis, J. Clin. Invest. 105 (2000) 1189–1197.
[19] A. Ito, Y. Koma, K. Uchino, T. Okada, C. Ohbayashi, N. Tsubota, M. Okada, Increased expression of connexin26 in the invasive component of lung squamous cell carcinoma: significant correlation with poor prognosis, Cancer Lett. 234 (2006) 239–248.
[20] Y. Naoi, Y. Miyoshi, T. Taguchi, S.J. Kim, T. Arai, Y. Tamaki, S. Noguchi, Connexin26 expression is associated with lymphatic vessel invasion and poor prognosis in human breast cancer, Breast Cancer Res. Treat. 106 (2007) 11–17.
[21] H. Yasuoka, Y. Nakamura, H. Zuo, W. Tang, Y. Takamura, A. Miyauchi, M. Nakamura, I. Mori, K. Kakudo, VEGF-D expression and lymph vessels play an important role for lymph node metastasis in papillary thyroid carcinoma, Mod. Pathol. 18 (2005) 1127–1133.
[22] Y. Kamibayashi, Y. Oyamada, M. Mori, M. Oyamada, Aberrant expression of gap junction proteins (connexins) is associated with tumor progression during multistage mouse skin carcinogenesis in vivo, Carcinogenesis 16 (1995) 1287–1297.
[23] M. Mourelle, F. Casellas, F. Guarner, A. Salas, V. Riveros-Moreno, S. Moncada, J.R. Malagelada, Induction of nitric oxide synthase in colonic smooth muscle from patients with toxic megacolon, Gastroenterology 109 (1995) 1497–1502.
[24] V. Krutovskikh, G. Mazzoleni, N. Mironov, Y. Omori, A.M. Aguelon, M. Mesnil, F. Berger, C. Partensky, H. Yamasaki, Altered homologous and heterologous gap-junctional intercellular communication in primary human liver tumors associated with aberrant protein localization but not gene mutation of connexin32, Int. J. Cancer 56 (1994) 87–94.
[25] H. Yamasaki, C.C. Naus, Role of connexin genes in growth control, Carcinogenesis 17 (1996) 1199–1213.

[26] Y. Omori, M.L. Zaidan Dagli, K. Yamakage, H. Yamasaki, Involvement of gap junctions in tumor suppression: analysis of genetically-manipulated mice, Mutat. Res. 477 (2001) 191–196.

[27] H. Xie, D.W. Laird, T.H. Chang, A mitosis-specific phosphorylation of the gap junction protein connexin43 in human vascular cells: biochemical characterization and localization, J. Cell Biol. 137 (1997) 203–210.

[28] T. Krenacs, M. Rosendaal, Immunohistological detection of gap junctions in human lymphoid tissue: connexin43 in follicular dendritic and lymphoendothelial cells, J. Histochem. Cytochem. 43 (1995) 1125–1137.

[29] L. Kanczuga-Koda, S. Sulkowski, A. Lenczewski, M. Koda, A. Wincewicz, M. Baltaziak, M. Sulkowska, Increased expression of connexin26 and 43 in lymph node metastases of breast cancer, J. Clin. Pathol. 59 (2006) 429–433.

J Cancer Res Clin Oncol (2009) 135:421–430
DOI 10.1007/s00432-008-0472-5

ORIGINAL PAPER

Association of loss of BRCA1 expression with centrosome aberration in human breast cancer

Atsushi Shimomura · Yasuo Miyoshi · Tetsuya Taguchi · Yasuhiro Tamaki · Shinzaburo Noguchi

Received: 16 June 2008 / Accepted: 1 September 2008 / Published online: 24 September 2008

Abstract
Purpose Centrosome aberration in number and/or size is reportedly often observed in human breast cancer. The aim of this study was to investigate the relationship between centrosome aberration and chromosomal instability as well as the expression of centrosome regulators such as BRCA1, Aurora-A, and p53.
Methods Centrosome aberration in number and size was determined immunohistochemically using the anti-γ-tubulin antibody, and chromosomal instability was evaluated by fluorescence in situ hybridization analysis of chromosomes 1, 11, and 17 in paraffin sections from 50 human breast cancers. Immunohistochemical examination of BRCA1, Aurora-A, and p53 was also performed to examine the relationship of their expression with centrosome aberration.
Results Percentage of tumor cells with centrosome aberration in size varied from 0.9 to 30.4% (median 9.5%) and in number it varied from 0.5 to 86.5% (median 34.5%) in each tumor. No significant association in number or size, however, was observed between chromosomal instability and centrosome aberration. Numerical centrosome aberration was significantly associated with negative BRCA1 expression ($P = 0.001$). Breast tumors ($n = 3$) from patients with a proven BRCA1 germline mutation also showed a significant relationship with numerical centrosome aberration ($P = 0.011$). On the other hand, expression of Aurora-A or p53 was not significantly associated with centrosome aberration in either number or size.
Conclusions Centrosome aberration is not associated with chromosomal instability, indicating the importance of other mechanisms in the induction of chromosomal instability in human breast cancer. BRCA1, but not Aurora-A and p53, is significantly involved in the pathogenesis of centrosome aberration.

Keywords Breast cancer · Centrosome amplification · Chromosomal instability · BRCA1 · Aurora-A

A. Shimomura · T. Taguchi · Y. Tamaki · S. Noguchi (✉)
Department of Breast and Endocrine Surgery,
Osaka University Graduate School of Medicine,
2-2 Yamadaoka, Suita, Osaka 565-0871, Japan
e-mail: noguchi@onsurg.med.osaka-u.ac.jp

Y. Miyoshi
Second Department of Surgery,
Hyogo College of Medicine, 1-1 Mukogawachou,
Nishinomiya, Hyogo 663-8131, Japan

Introduction

Centrosome, as a major microtubule organization center, regulates the number, stability, polarity, and arrangement of microtubules in interphase cells (Rose et al. 1993; Kellogg et al. 1994). Duplication of centrosomes occurs once in each cell cycle (Stearns 2001). During G2-M phase transition, replicated centrosomes separate to form a bipolar mitotic spindle (Kellogg et al. 1994; Meraldi et al. 1999). Failure of centrosome duplication and DNA replication to synchronize may lead to segregation errors of chromosomes at cell division, culminating in chromosomal instability (Brinkley and Goepfert 1998; Orr-Weaver and Weinberg 1998; Ghadimi et al. 2000). Centrosome aberration, as well as chromosomal instability, is reportedly often observed in human breast cancers (Pihan et al. 1998). It is speculated that centrosome aberration induces chromosomal instability through the development of multipolar mitotic spindles. Extra centrosomes, however, do not always lead to multipolarity as a result of centrosomal clustering, which prevents the formation of multipolar spindles

and chromosomal instability (Quintyne et al. 2005). A few studies have been reported on the association between centrosome aberration and chromosomal instability in human breast cancer, but the results appear to be inconsistent since using different methodologies for the determination of centrosome aberration and chromosomal instability has resulted in reports of both a positive and a negative association (Lingle et al. 2002; Schneeweiss et al. 2003; Kronenwett et al. 2005).

Centrosome function is regulated by multiple factors (Sankaran and Parvin 2006), among which BRCA1 has recently been attracting considerable attention. Although BRCA1 has various functions such as DNA repair, transcriptional regulation, cell-cycle checkpoint control, and protein ubiquitination (Deng 2002; Parvin 2004), recent studies have disclosed that BRCA1 interacts with a variety of proteins that regulate centrosome duplication and that the targeted disruption of BRCA1 results in centrosome amplification, which indicates that BRCA1 serves as a negative regulator for centrosome duplication (Deng 2002; Starita et al. 2004). BRCA1 germline mutations account for about 40% of familial breast cancer cases, whereas BRCA1 is rarely mutated in sporadic breast cancer (Deng and Brodie 2000; Deng 2002). However, both mRNA and protein expression of BRCA1 are downregulated in as much as around 30% of sporadic breast cancer cases, mostly due to the acquired methylation of the BRCA1 promoter or malfunctions in the upstream pathways that regulate BRCA1 expression (Yang et al. 2001), indicating that this gene has an important role in the pathogenesis of sporadic breast cancer as well. Although recent studies using breast cancer cell lines have shown that BRCA1 regulates centrosome dynamics and that loss of BRCA1 leads to centrosome aberration (Parvin and Sankaran 2006), there has been no report until now which investigates this association in human breast cancer tissues. It therefore seemed to be of considerable interest to examine whether BRCA1 is involved in the induction of centrosome aberration in sporadic breast cancer.

In the study presented here, we therefore studied the centrosome aberration in human breast cancer and tried to identify the clinicopathological features of tumors with centrosome aberration as well as the relationship of such aberration with chromosomal instability. In addition, the associations between centrosome aberration and expression of BRCA1, Aurora-A, and p53 were investigated.

Materials and methods

Tissue specimens

Breast cancer tissues were obtained from 50 primary (sporadic) breast cancer patients who underwent surgery at Osaka University Hospital between 2004 and 2006 (47 invasive ductal carcinomas, one mucinous carcinoma, one invasive lobular carcinoma, and one apocrine carcinoma). Normal breast tissues ($n = 7$) adjacent to tumor tissues were also obtained. All surgical specimens were fixed in 10% buffered formalin and embedded in paraffin. Informed consent as to this study was obtained from each patient before surgery.

Fluorescence in situ hybridization

Fluorescence in situ hybridization (FISH) was performed according to the manufacturer's instructions (Vysis/Abbott Molecular Inc., Des Plaines, IL), with minor modifications. Tissue sections (6 μm) applied to silanized slides were baked overnight at 60°C. Three-color FISH was used for the simultaneous detection of chromosomes 1, 11, and 17. Pretreatment was performed with the Paraffin Pretreatment Kit (Vysis/Abbott Molecular Inc.) according to the manufacturer's instructions with minor modifications. We prolonged the time for treatment with Protease Buffer (Vysis/Abbott Molecular Inc.) from 10 to 60 min, and added BSA (Sigma, St Louis, MO) to a mixture of CEP Hybridization Buffer (Vysis/Abbott Molecular Inc.) and three centromere probes, CEP 1, CEP 11, and CEP 17 (Vysis/Abbott Molecular Inc.). For counterstaining, sections were incubated for 5 min in a wash buffer with Hoechst 33258 (1:10,000; Invitrogen, Carlsbad, CA) instead of DAPI II (Vysis/Abbott Molecular Inc.). Furthermore, we used Prolong Gold Antifade Reagent (Invitrogen) on slide-mounted specimens for covering with the coverslips.

Nuclei, Ch1 orange signals, Ch11 green signals, and Ch17 blue signals were detected with an AX80 microscope (Olympus, Tokyo, Japan) equipped with a DAPI/Green/Orange triple band-pass filter set and a Blue filter set (both Vysis/Abbott Molecular Inc.) to detect. For data collection, three or four microscopic areas were selected (60 objectives), and three-dimensional image stacks, each consisting of 12 planes at a distance of 0.5 μm on the z-axis, were identified microscopically with each of the two band-pass filters. The two image stacks with each two band-pass filters were then converted into two corresponding projection images of all recorded slices and finally processed with WinROOF image processing software (Mitani Corporation, Tokyo, Japan) into one image with nuclei and three signal colors. Only signals in non-overlapping, intact nuclei were evaluated, while hybridization signals were counted in at least 200 interphase nuclei. We also calculated the chromosomal instability value (CIN value), defined by Lengauer et al. as the percentage of cells with a nonmodal chromosome (Lengauer et al. 1997).

Centrosome labeling and determination of aberration

Tissue sections (6 μm) were deparaffinized and hydrated with standard procedures. Antigens were retrieved by heating the samples in Target Retrieval Solution (pH6.0; Dako, Kyoto, Japan) at 95°C for 40 min. After treatment with Block Ace (Dainippon Sumitomo Pharmaceutical, Osaka, Japan) for 30 min at room temperature, the sections were incubated with a primary mouse anti-γ-tubulin antibody (1:300, clone GTU-88; Sigma, St Louis, MO), followed by incubation with a Cy-3-conjugated Affinipure F(ab')2 Fragment Donkey Anti Mouse IgG (H + L) (1:100; Jackson Immunoresearch, West Grove, PA) and Hoechst 33258 (1:10,000; Invitrogen) for 1 h at room temperature. Image stacks including nuclei and γ-tubulin centrosome signals (red) were acquired with an AX80 microscope and processed into one projection image with the same method as used for FISH.

Centrosome images of normal breast tissues were used as controls. A normal centrosome was defined as one or two regularly rounded spots of uniform size and shape. A tumor cell with three or more centrosomes was considered to have an aberration in centrosome number. We calculated the percentage of tumor cells with centrosome aberration in size by examining at least 200 cells per tumor as well as the size of the centrosomes. A tumor cell with at least one centrosome measuring more than three SDs above the average size of control centrosomes from normal breast tissues was considered as to have an aberration in centrosome size. In addition to the 50 sporadic breast cancers, the number and size of centrosomes in BRCA1-associated hereditary breast cancers from three patients with a proven BRCA1 germline mutation (470delCT, 3453insGGCTA, and 3493delCT, respectively) were also analyzed.

Immunohistochemistry of BRCA1, Aurora-A, and p53

Tissue sections (3 μm) were deparaffinized, hydrated with standard procedures, and subjected to immunohistochemical staining of BRCA1, Auora-A, and p53 protein with the avidin–biotin immunoperoxidase method. In brief, for BRCA1 staining, the antigen was retrieved by heating in a microwave oven at 500 W for 15 min in Target Retrieval Solution (pH 6.0; Dako). For Aurora-A and p53 staining, the antigens were retrieved by heating the samples in Target Retrieval Solution at 95°C for 40 min. Endogeneous peroxidases were quenched by incubating the sections for 20 min in 3% H_2O_2. After treatment with Block Ace for 30 min at room temperature, slides were then incubated with the primary antibodies BRCA1(Ab-1) antibody (1:70; Calbiochem, San Diego, CA), Aurora-A antibody (1:200; TransGenic, Kumamoto, Japan) or p53(DO-7) antibody (1:100; Dako) at 4°C overnight and diluted with phosphate-buffered saline (PBS) containing 0.3% Tween 20 (vol/vol).

For BRCA1 or p53 staining, tumor cells with nuclear staining were considered positive, and for Aurora-A staining, those with cytoplasmic staining were considered positive. A BX51 microscope (Olympus) was used to count 1,000 tumor cells from each case. When tumor cells positive for BRCA1, p53, or Aurora-A staining were observed in more than 10% of the cells, the tumor was considered positive for the respective molecule.

Estrogen receptor and progesterone receptor assay

Estrogen receptor (ER) and progesterone receptor (PR) contents of breast cancer tissues were determined immunohistochemically, with staining of 10% or more of the nucleus of a cancer cell resulting in a classification as positive.

Human epidermal growth receptor-2 FISH analysis

Human epidermal growth receptor-2 (HER2) amplification was determined with the FISH method using the PathVysion HER-2 DNA Probe Kit (Vysis/Abbott Molecular Inc.). FISH scoring was performed by counting fluorescence signals in at least 60 malignant cell nuclei per case, and for each specimen, the ratio of HER2 gene signals to chromosome 17 centromere signals was calculated. A tumor was considered to be HER2-amplified if the FISH ratio was ≥ 2.0.

Statistics

The relationship between clinicopathological parameters and centrosome aberration or chromosomal instability was analyzed with Mann–Whitney's U test. Chi-square test was used for analysis of the relationship between clinicopathological parameters and BRCA1, Aurora-A, or p53 expression. Spearman coefficients for the correlation between chromosomal instability and centrosome aberration in size and number were also calculated. Statistical significance was defined as $P < 0.05$. SPSS software (SPSS Inc., Chicago, IL) was used for all statistical analyses.

Results

Centrosome aberration

Since the average centrosome size of normal epithelial cells was 0.91 ± 0.12 μm ($n = 7$), centrosomes larger than 1.27 μm (average + 3 SD) were considered to be centrosomes with aberration in size. Of the 50 breast cancers, the percentage of tumor cells with centrosome aberration in

size varied from 0.9 to 30.4% (median 9.5%) in each tumor, and that of tumor cells with centrosome aberration in number (≥3) from 0.5 to 86.5% (median 34.5%) in each tumor. Representative results of breast cancers with centrosome aberrations in number or in both number and size are shown in Fig. 1a–f and those of normal breast epithelial cells are also shown in Fig. 1g–i.

Relationships between clinicopathological parameters and centrosome aberration are shown in Table 1. Centrosome aberration in either number or size showed no significant association with any of the clinicopathological parameters of age, tumor size, nodal status, ER status, PR status, histological grade, and HER2 amplification.

Chromosomal instability

The copy numbers of chromosomes 1, 11, and 17 of the 50 breast cancers were determined with three-color FISH. The CIN value for each of these chromosomes was defined according to Lengauer et al.'s criteria as the percentage of tumor cells with a nonmodal chromosome (Lengauer et al. 1997). CIN values were then calculated for each of the three chromosomes, and the average of these values was finally adopted as the CIN value of the tumor. CIN values of the breast cancers varied from 34.2 to 69.5% (median 57.3%), with representative FISH results shown in Fig. 2.

The relationship between clinicopathological parameters and chromosomal instability is shown in Table 2. Chromosomal instability was significantly associated with large tumor size ($P = 0.005$) and marginally significantly associated with high histological grade ($P = 0.050$). No significant association was observed between chromosomal instability and age, nodal status, ER status, PR status, or HER2 amplification.

Correlation between centrosome aberration and chromosomal instability

Figure 3 shows correlation of centrosome aberration in number or in size with chromosomal instability. No significant

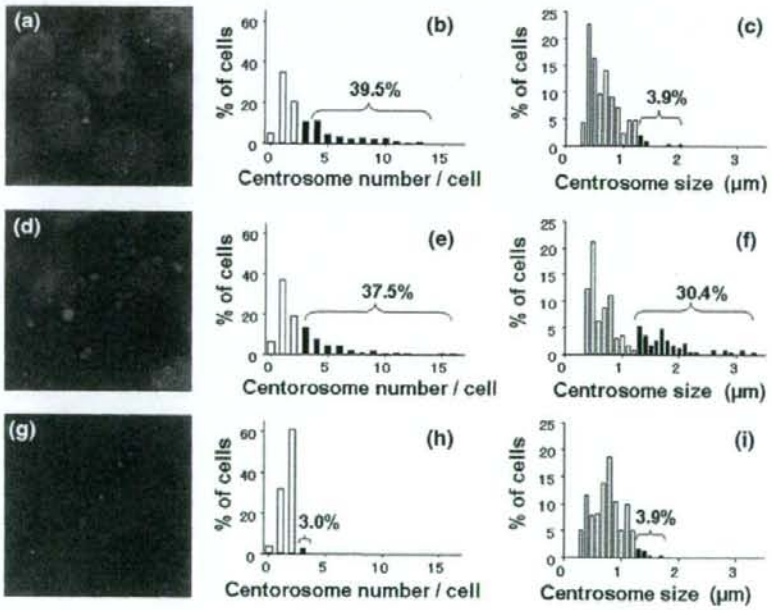

Fig. 1 Representative results of immunohistochemical analysis of centrosomes. Immunohistochemical staining of centrosomes with monoclonal anti-γ-tubulin antibody (**a**, **d**, **g**) and histograms of percentages of tumor cells with various numbers (**b**, **e**, **h**) and sizes (**c**, **f**, **i**) of centrosomes. Percentages of tumor cells with centrosome number ≥3 are shown in *solid bars* (**b**, **e**, **f**) as are those with centrosome measuring >1.27 μm (**c**, **f**, **i**). Breast cancer with centrosome aberration in number (**a**). Percentages of tumor cells with centrosome aberration in number and in size were 39.5 and 3.9%, respectively (**b**, **c**). Breast cancer with centrosome aberration in both number and size (**d**). Percentages of tumor cells with centrosome aberration in number and size were 37.5 and 30.4% respectively (**e**, **f**). Normal breast tissue (**g**). Percentages of normal cells with centrosome aberration in number and size were 3.0 and 3.9%, respectively (**h**, **i**)

Table 1 Relationship between centrosome aberration and clinicopathological parameters

Variable	Number of tumors	Percentage of cells with centrosome aberration							
		Number				Size			
		Median	Mean	95% CI	*P* value	Median	Mean	95% CI	*P* value
Age (years)					0.623				0.357
<50	17	34.5	37.9	25.7–50.0		10.3	12.9	8.4–17.4	
≥50	33	34.5	32.1	25.4–38.9		8.9	10.3	7.9–12.7	
Tumor size					0.806				0.366
<2 cm	29	34.5	35.4	26.9–44.0		10.0	11.5	9.0–14.0	
≥2 cm	21	34.5	32.2	23.9–40.5		8.4	10.7	6.8–14.7	
Nodal status					0.266				1.000
Negative	38	34.5	36.1	29.2–43.0		9.5	10.9	8.7–13.2	
Positive	12	32.8	27.6	15.5–39.7		9.0	11.9	6.0–17.8	
ER status					0.266				0.412
Negative	8	23.5	27.4	9.0–45.8		7.5	9.1	4.3–13.9	
Positive	42	34.8	35.3	29.0–41.7		9.6	11.6	9.1–14.0	
PR status					0.653				0.327
Negative	19	32.0	32.2	21.8–42.6		10.0	12.0	8.6–15.4	
Positive	31	34.5	35.2	27.8–42.7		8.9	10.7	7.8–13.6	
Histological grade					0.294				0.953
1	20	35.5	38.2	27.7–48.8		9.5	11.1	7.7–14.4	
2 and 3	30	32.3	31.3	24.1–38.5		9.3	11.3	8.3–14.2	
HER2 amplification					0.690				0.665
Negative	39	32.5	33.8	26.8–40.8		10.7	11.0	8.8–13.2	
Positive	11	37.5	35.2	23.2–47.1		8.2	11.9	5.2–18.6	

correlation was observed for either number (Spearman $r = -0.113$, $P = 0.436$) or size (Spearman $r = -0.160$, $P = 0.268$).

Relationship between centrosome aberration and BRCA1, Aurora-A, or p53 expression

Representative results of immunohistochemical staining for BRCA1, Aurora-A, and p53 are shown in Fig. 4. BRCA1, Aurora-A, and p53 were positive in 18 (36%), 9 (18%), and 16 (32%) breast cancers, respectively.

The percentage of tumor cells with centrosome aberration in number was significantly larger for BRCA1-negative than for BRCA1-positive tumors ($P = 0.001$), whereas there was no significant difference between the two groups in the percentage of tumor cells with centrosome aberration in size (Fig. 5). In addition, we analyzed centrosome aberration in BRCA1-associated hereditary breast cancers, which were obtained from patients with a proven BRCA1 germline mutation. These breast tumors showed a significantly higher percentage of tumor cells with centrosome aberration in number ($P = 0.011$) and a significantly lower percentage of tumor cells with centrosome aberration in size ($P = 0.017$) than BRCA-positive tumors. The expression status of Aurora-A as well as p53 was not significantly associated with centrosome aberration in number or in size.

Relationship between chromosomal instability and BRCA1, Aurora-A, or p53 expression

Relationship between chromosomal instability and BRCA1, Aurora-A, or p53 expression is shown in Fig. 6. Aurora-A expression, but not BRCA1 or p53 expression, was significantly associated with chromosomal instability ($P = 0.003$).

Relationship between clinicopathological parameters and BRCA1, Aurora-A, or p53 expression

BRCA1, Aurora-A, and p53 expression were studied immunohistochemically, and their relationship with various clinicopathological parameters is shown in Table 3. There is no significant correlation between clinicopathological parameters and BRCA1 expression. Positive expression of Aurora-A significantly correlated with negative ER status ($P = 0.003$) and negative PR status ($P = 0.001$), and positive expression of p53 significantly correlated with HER2 amplification ($P = 0.024$).

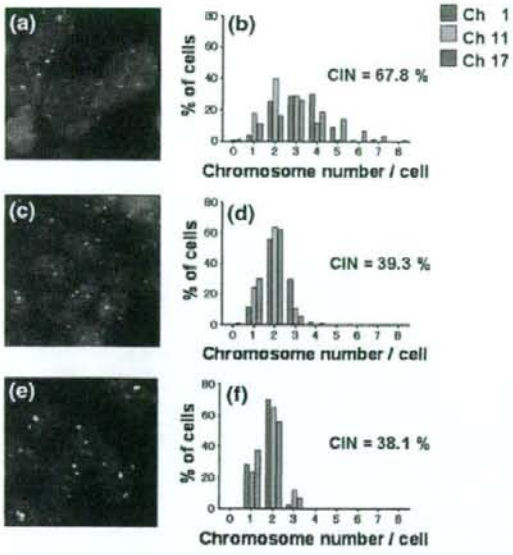

Fig. 2 Representative results of chromosomal instability FISH analysis. Three-color FISH images for chromosomes 1 (*orange*), 11 (*green*), and 17 (*blue*) (**a**, **c**, **e**) and histograms of tumor cells with various numbers of each chromosome (**b**, **d**, **f**). Breast cancer with high chromosomal instability (CIN = 67.8%) (**a**, **b**). Breast cancer with low chromosomal instability (CIN = 39.3%) (**c**, **d**). Normal breast tissue (CIN = 38.1%) (**e**, **f**)

Table 2 Relationship between chromosomal instability and clinicopathological parameters

Variable	Number of tumors	Chromosomal instability			
		Median	Mean	95% CI	*P* value
Age (years)					0.705
< 50	17	56.8	56.7	52.0–61.5	
≥ 50	33	57.8	54.9	51.3–58.5	
Tumor size					0.005
< 2 cm	29	55.7	52.1	48.1–56.1	
≥ 2 cm	21	61.7	60.2	57.4–63.0	
Nodal status					0.794
Negative	38	57.8	55.6	52.3–58.8	
Positive	12	56.9	55.4	49.1–61.7	
ER status					0.168
Negative	8	58.9	60.1	56.4–63.8	
Positive	42	56.9	54.6	51.4–57.8	
PR status					0.322
Negative	19	58.2	57.2	52.9–61.6	
Positive	31	57.0	54.5	50.7–58.2	
Histological grade					0.050
1	20	53.1	52.2	47.5–56.9	
2 and 3	30	58.3	57.7	54.3–61.1	
HER2 amplification					0.228
Negative	39	57.2	54.7	51.5–57.9	
Positive	11	59.0	58.5	52.4–64.5	

Discussion

The findings of our study confirmed those of previous reports that centrosome aberration is a common phenomenon in human breast cancers. Tumor cells with centrosome aberration in number and/or size were observed essentially in all breast tumors analyzed, although the range of percentages of tumor cells with centrosome aberration varied widely from tumor to tumor. We attempted to elucidate the relationship between centrosome aberration and other clinicopathological characteristics of breast tumors. Some reports have dealt with the association between centrosome aberration and lymph node status, ER, PR, or HER2, but the findings were not consistent (Schneeweiss et al. 2003; Kronenwett et al. 2005; Guo et al. 2007). Our study also failed to identify a significant association between centrosome aberration and any of the conventional clinicopathological parameters of menopausal status, tumor size, lymph node status, histological grade, ER status, PR status, or HER2 status. We therefore believe that centrosome aberration is not associated, or at least not significantly, with conventional clinicopathological parameters. On the other hand, chromosomal instability showed a significant association with tumor size ($P = 0.005$) and a borderline

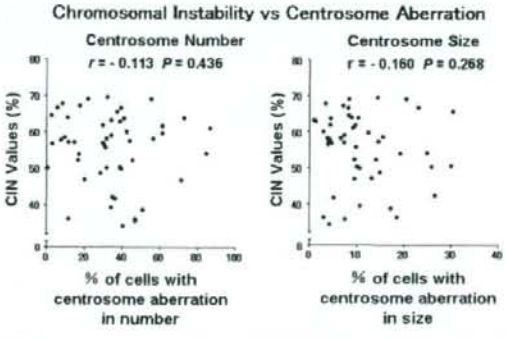

Fig. 3 Correlation between chromosomal instability (CIN) and centrosome aberration in number or size

significance with high histological grade ($P = 0.050$), findings consistent with those of a previous report (Takami et al. 2001).

The possibility that centrosome aberration is associated with chromosomal instability has been introduced (Salisbury et al. 2004), but the relevant results have not been consistent (Lingle et al. 2002; Schneeweiss et al. 2003; Kronenwett et al. 2005), while our study did not find a significant

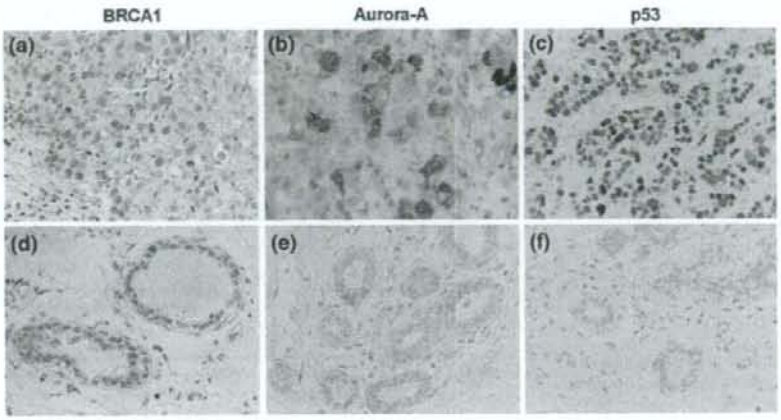

Fig. 4 Representative results of immunohistochemistry of BRCA1, Aurora-A, and p53 (×400). Positive BRCA1 staining in cancer cells (**a**) and in adjacent normal breast epithelial cells (**d**). Positive Aurora-A staining in cancer cells (**b**), and negative Aurora-A staining in adjacent normal breast epithelial cells (**e**). Positive p53 staining in cancer cells (**c**), and negative p53 staining in adjacent normal breast epithelial cells (**f**)

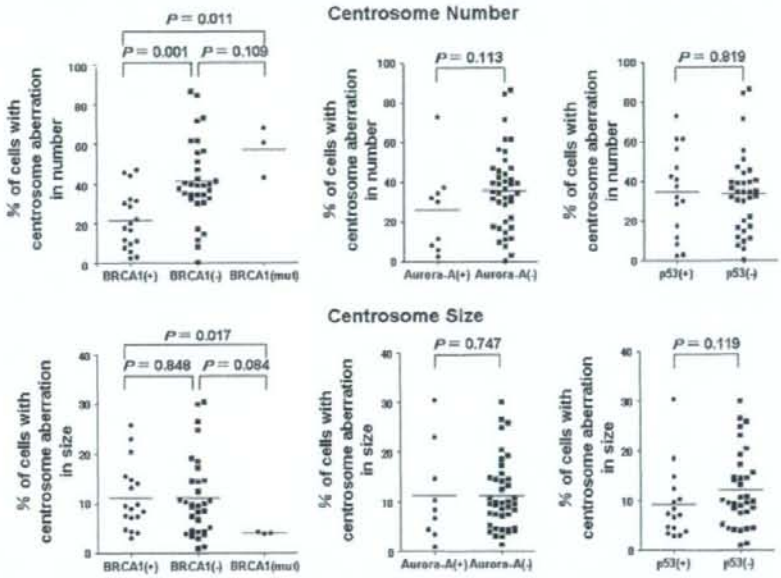

Fig. 5 Relationship between centrosome aberration and expression of BRCA1, Aurora-A, and p53. Centrosome aberrations in number (*upper panels*) and size (*lower panels*) were compared according to the expression status of BRCA1, Aurora-A, and p53. BRCA1 (mut); BRCA1-associated hereditary breast cancers. *Red bars* mean

association between these two factors. It therefore appears that centrosome aberration is not a major determinant of abnormal chromosomal segregation leading to chromosomal instability in human breast cancer. Similarly, centrosome aberration in a Burkitt's lymphoma reportedly did not result in chromosomal instability (Duensing et al. 2003). It is speculated that excessive centrosomes are nonfunctional and thus do not participate in chromosome segregation. Moreover, centrosome inactivation may occur in cells with an abnormal number of centrosomes to prevent abnormal chromosome segregation (Sibon et al. 2000). Sluder and Nordberg have proposed an alternative mechanism, i.e., spindle-pole bundling in cells with multiple centrosomes coalescence, which may lead to bipolar division so that chromosome segregation remains equal (Sluder and Nordberg 2004). In this study, we observed an interesting image of cell division as shown in Fig. 7, i.e., a dividing cell with centrosome coalescence. The centrosomes coalesce to form a pole in each daughter cell and chromosomes appear to be equally segregated. Furthermore, a recent study has introduced the possibility that centrosome clustering prevents the formation of multipolar spindles (Quintyne et al. 2005). It is thought that formation of multiple spindle-poles appears to need two steps, i.e., an increase in centrosome number and an inhibition of centrosomal coalescence (Quintyne et al. 2005). Therefore, the presence

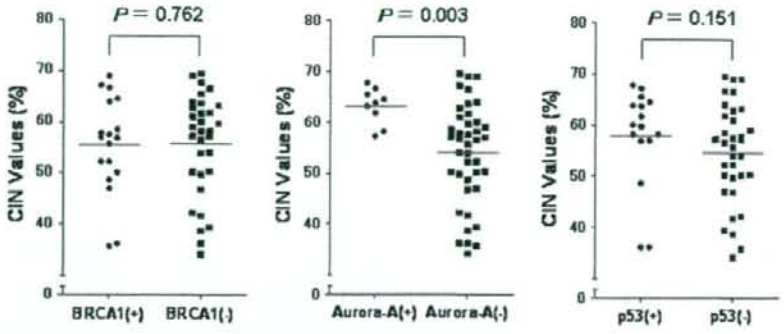

Fig. 6 Relationship between chromosomal instability and expression of BRCA1, Aurora-A, and p53. Chromosomal instability was compared according to the expression status of BRCA1, Aurora-A, and p53. *Red bars* mean

Table 3 Relationship between clinicopathological parameters and BRCA1, Aurora-A, or p53 expression

Variable	Number of tumors	BRCA1			Aurora-A			p53		
		−	+	*P* value	−	+	*P* value	−	+	*P* value
Age (years)				0.227			1.000			0.053
<50	17	13	4		14	3		15	2	
≥50	33	19	14		27	6		19	14	
Tumor size				0.774			1.000			0.543
<2 cm	29	18	11		24	5		21	8	
≥2 cm	21	14	7		17	4		13	8	
Nodal status				1.000			1.000			1.000
Negative	38	24	14		31	7		26	12	
Positive	12	8	4		10	2		8	4	
ER status				0.231			0.003			0.092
Negative	8	7	1		3	5		3	5	
Positive	42	25	17		38	4		31	11	
PR status				0.130			0.001			0.349
Negative	19	15	4		11	8		11	8	
Positive	31	17	14		30	1		23	8	
Histological grade				0.134			0.067			0.062
1	20	10	10		19	1		17	3	
2 and 3	30	22	8		22	8		17	13	
HER2 amplification				0.287			0.392			0.024
Negative	39	23	16		33	6		30	9	
Positive	11	9	2		8	3		4	7	

of centrosome aberration does not necessarily lead to subsequent chromosomal instability. For this reason, future studies are needed of the precise function of centrosomal coalescence.

Recent studies have disclosed an important role of BRCA1 in centrosome duplication. Mouse embryonic fibroblast cells carrying a targeted deletion of exon 11 of the Brca1 gene have been found to maintain an intact G1-S cell cycle checkpoint but to have a defective G2-M checkpoint. These cells contain multiple, functional centrosomes, which lead to unequal chromosome segregation, abnormal nuclear division, and aneuploidy (Xu et al. 1999). Moreover, BRCA1-dependent ubiquitination of γ-tubulin is thought to be involved in the regulation of centrosome number (Starita et al. 2004). It can therefore be hypothesized that BRCA1 also plays an important role in centrosome duplication in human breast cancer, although no studies on this issue have been published yet. We were able to show that BRCA1-negative expression is significantly associated with centrosome aberration in number and, in addition, that all three BRCA1-associated hereditary breast cancers in our study also had centrosome aberration in number. These results strongly indicate that BRCA1 plays an important role in the regulation of centrosome duplication, and loss of its expression results in numerical centrosome aberration.

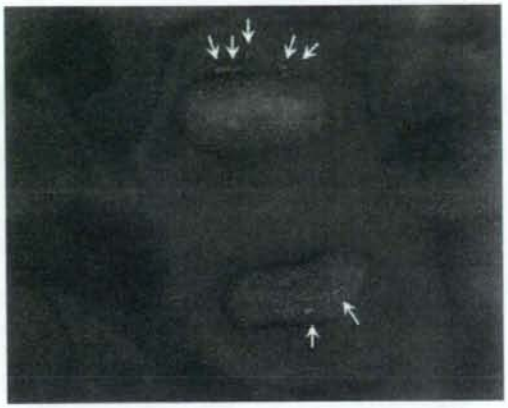

Fig. 7 Representative image of centrosome coalescence. This picture shows a cell with numerous centrosomes, which is dividing into two cells. The centrosomes coalesce to form a pole in each daughter cell and chromosomes appear to be equally segregated. *Arrows* indicate centrosomes

Interestingly, all three BRCA1-associated hereditary breast cancers showed a significantly smaller percentage of tumor cells with centrosome aberration in size than did BRCA1-positive breast cancers (Fig. 5), indicating that the average centrosome size is smaller in BRCA1-associated breast cancers than in BRCA1-positive breast cancers. Startia et al. reported that Hs578T breast cancer cells, when the BRCA1 function is inhibited with the BRCA1-interfering peptide fragment, frequently show numerous centrosomes with only one centriole due to centrosome fragmentation (Starita et al. 2004). The small centrosome size in BRCA1-associated breast cancers observed in our study seems to suggest the presence of such a centrosome fragmentation. On the other hand, centrosome size appears to be similar in BRCA1-positive and -negative sporadic breast cancers, but the reason why it is not smaller in BRCA1-negative than in BRCA1-positive sporadic tumors is currently unknown. The role of BRCA1 loss in the formation of centrosome aberration in sporadic breast cancers thus needs to be studied in more detail.

Since Aurora-A has been shown to perform an important function in centrosome duplication in both in vitro and in vivo studies, it was expected that Aurora-A expression would be associated with centrosome aberration in human breast cancers as well. However, we could not find any significant association in our study, but the reason for this lack of association in human breast cancers is currently unknown. However, the fact that centrosome aberration was often observed in Aurora-A-negative tumors seems to indicate that other factors, including BRCA1, play a more important role in the pathogenesis of centrosome aberration in human breast cancers. On the other hand, Aurora-A expression was found to be associated with chromosomal instability, as it was in a previous study of ours (Miyoshi et al. 2001). Aurora-A has various functions other than the regulation of centrosome function, and Aurora-A overexpression can cause the cells with chromosomal abnormalities to override the spindle checkpoint (Dutertre and Prigent 2003), resulting in chromosomal instability. We therefore speculate that chromosomal instability in Aurora-A-positive breast tumors is induced by Aurora-A through a pathway, which does not induce centrosome aberration in human breast cancers.

p53 plays a key role in mediating cell response to various types of stress, mainly by inducing or repressing a number of genes involved in cell cycle, senescence, apoptosis, DNA repair, and angiogenesis (Lacroix et al. 2006). It was also demonstrated that, in mouse embryonic fibroblasts (MEFs) lacking p53, multiple copies of functionally competent centrosomes are generated during a single cell cycle (Fukasawa et al. 1996). p53 controls centrosome duplication through transcriptional regulation of the cyclin-dependent kinase inhibitor $p21^{Waf1/Cip1}$ and its subsequent inhibition of CDK/cyclin E activity, which is involved in the initiation of centrosome duplication (Mussman et al. 2000; Tarapore et al. 2001). In our study, however, no significant association between p53 status and centrosome aberration was observed, which is consistent with the finding of a previous study (Lingle et al. 2002), indicating that p53 seems not to play a role, or at least not a major role, in the pathogenesis of centrosome aberration in human breast cancers.

In conclusion, we have shown that centrosome aberration in number or size is often observed in human breast cancers but that it is not significantly associated with chromosomal instability. This indicates the importance of other mechanisms such as spindle checkpoint abnormalities in the induction of chromosomal instability. BRCA1, but not Aurora-A or p53, is significantly implicated in the pathogenesis of centrosome aberration. Our observations need to be confirmed by a study comprising a larger number of breast tumors. In addition, not only the number or size of centrosomes but also their function needs to be studied in greater detail in future.

Conflict of interest statement There is no conflict of interest to declare in relation to this manuscript.

References

Brinkley BR, Goepfert TM (1998) Supernumerary centrosomes and cancer: Boveri's hypothesis resurrected. Cell Motil Cytoskeleton 41(4):281–288. doi:10.1002/(SICI)1097-0169(1998)41:4<281::AID-CM1>3.0.CO;2-C

Deng CX (2002) Roles of BRCA1 in centrosome duplication. Oncogene 21(40):6222–6227. doi:10.1038/sj.onc.1205713

Deng CX, Brodie SG (2000) Roles of BRCA1 and its interacting proteins. Bioessays 22(8):728–737. doi:10.1002/1521-1878(200008)22:8<728::AID-BIES6>3.0.CO;2-B

Duensing S, Lee BH, Dal Cin P, Munger K (2003) Excessive centrosome abnormalities without ongoing numerical chromosome instability in a Burkitt's lymphoma. Mol Cancer 2:30. doi:10.1186/1476-4598-2-30

Dutertre S, Prigent C (2003) Aurora-A overexpression leads to override of the microtubule-kinetochore attachment checkpoint. Mol Interv 3(3):127–130. doi:10.1124/mi.3.3.127

Fukasawa K, Choi T, Kuriyama R, Rulong S, Vande Woude GF (1996) Abnormal centrosome amplification in the absence of p53. Science 271(5256):1744–1747. doi:10.1126/science.271.5256.1744

Ghadimi BM, Sackett DL, Difilippantonio MJ, Schrock E, Neumann T, Jauho A et al (2000) Centrosome amplification and instability occurs exclusively in aneuploid, but not in diploid colorectal cancer cell lines, and correlates with numerical chromosomal aberrations. Genes Chromosomes Cancer 27(2):183–190. doi:10.1002/(SICI)1098-2264(200002)27:2<183::AID-GCC10>3.0.CO;2-P

Guo HQ, Gao M, Ma J, Xiao T, Zhao LL, Gao Y et al (2007) Analysis of the cellular centrosome in fine-needle aspirations of the breast. Breast Cancer Res 9(4):R48. doi:10.1186/bcr1752

Kellogg DR, Moritz M, Alberts BM (1994) The centrosome and cellular organization. Annu Rev Biochem 63:639–674. doi:10.1146/annurev.bi.63.070194.003231

Kronenwett U, Huwendiek S, Castro J, Ried T, Auer G (2005) Characterisation of breast fine-needle aspiration biopsies by centrosome aberrations and genomic instability. Br J Cancer 92(2):389–395. doi:10.1038/sj.bjc.6602246

Lacroix M, Toillon RA, Leclercq G (2006) p53 and breast cancer, an update. Endocr Relat Cancer 13(2):293–325. doi:10.1677/erc.1.01172

Lengauer C, Kinzler KW, Vogelstein B (1997) Genetic instability in colorectal cancers. Nature 386(6625):623–627. doi:10.1038/386623a0

Lingle WL, Barrett SL, Negron VC, D'Assoro AB, Boeneman K, Liu W et al (2002) Centrosome amplification drives chromosomal instability in breast tumor development. Proc Natl Acad Sci USA 99(4):1978–1983. doi:10.1073/pnas.032479999

Meraldi P, Lukas J, Fry AM, Bartek J, Nigg EA (1999) Centrosome duplication in mammalian somatic cells requires E2F and Cdk2-cyclin A. Nat Cell Biol 1(2):88–93. doi:10.1038/10054

Miyoshi Y, Iwao K, Egawa C, Noguchi S (2001) Association of centrosomal kinase STK15/BTAK mRNA expression with chromosomal instability in human breast cancers. Int J Cancer 92(3):370–373. doi:10.1002/ijc.1200

Mussman JG, Horn HF, Carroll PE, Okuda M, Tarapore P, Donehower LA et al (2000) Synergistic induction of centrosome hyperamplification by loss of p53 and cyclin E overexpression. Oncogene 19(13):1635–1646. doi:10.1038/sj.onc.1203460

Orr-Weaver TL, Weinberg RA (1998) A checkpoint on the road to cancer. Nature 392(6673):223–224. doi:10.1038/32520

Parvin JD (2004) Overview of history and progress in BRCA1 research: the first BRCA1 decade. Cancer Biol Ther 3(6):505–508

Parvin JD, Sankaran S (2006) The BRCA1 E3 ubiquitin ligase controls centrosome dynamics. Cell Cycle 5(17):1946–1950

Pihan GA, Purohit A, Wallace J, Knecht H, Woda B, Quesenberry P et al (1998) Centrosome defects and genetic instability in malignant tumors. Cancer Res 58(17):3974–3985

Quintyne NJ, Reing JE, Hoffelder DR, Gollin SM, Saunders WS (2005) Spindle multipolarity is prevented by centrosomal clustering. Science 307(5706):127–129. doi:10.1126/science.1104905

Rose MD, Biggins S, Satterwhite LL (1993) Unravelling the tangled web at the microtubule-organizing center. Curr Opin Cell Biol 5(1):105–115. doi:10.1016/S0955-0674(05)80015-8

Salisbury JL, D'Assoro AB, Lingle WL (2004) Centrosome amplification and the origin of chromosomal instability in breast cancer. J Mammary Gland Biol Neoplasia 9(3):275–283. doi:10.1023/B:JOMG.0000048774.27697.30

Sankaran S, Parvin JD (2006) Centrosome function in normal and tumor cells. J Cell Biochem 99(5):1240–1250. doi:10.1002/jcb.21003

Schneeweiss A, Sinn HP, Ehemann V, Khbeis T, Neben K, Krause U et al (2003) Centrosomal aberrations in primary invasive breast cancer are associated with nodal status and hormone receptor expression. Int J Cancer 107(3):346–352. doi:10.1002/ijc.11408

Sibon OC, Kelkar A, Lemstra W, Theurkauf WE (2000) DNA-replication/DNA-damage-dependent centrosome inactivation in Drosophila embryos. Nat Cell Biol 2(2):90–95. doi:10.1038/35000041

Sluder G, Nordberg JJ (2004) The good, the bad and the ugly: the practical consequences of centrosome amplification. Curr Opin Cell Biol 16(1):49–54. doi:10.1016/j.ceb.2003.11.006

Starita LM, Machida Y, Sankaran S, Elias JE, Griffin K, Schlegel BP et al (2004) BRCA1-dependent ubiquitination of gamma-tubulin regulates centrosome number. Mol Cell Biol 24(19):8457–8466. doi:10.1128/MCB.24.19.8457-8466.2004

Stearns T (2001) Centrosome duplication. a centriolar pas de deux. Cell 105(4):417–420. doi:10.1016/S0092-8674(01)00366-X

Takami S, Kawasome C, Kinoshita M, Koyama H, Noguchi S (2001) Chromosomal instability detected by fluorescence in situ hybridization in Japanese breast cancer patients. Clin Chim Acta 308(1/2):127–131. doi:10.1016/S0009-8981(01)00473-9

Tarapore P, Horn HF, Tokuyama Y, Fukasawa K (2001) Direct regulation of the centrosome duplication cycle by the p53-p21Waf1/Cip1 pathway. Oncogene 20(25):3173–3184. doi:10.1038/sj.onc.1204424

Xu X, Weaver Z, Linke SP, Li C, Gotay J, Wang XW et al (1999) Centrosome amplification and a defective G2-M cell cycle checkpoint induce genetic instability in BRCA1 exon 11 isoform-deficient cells. Mol Cell 3(3):389–395. doi:10.1016/S1097-2765(00)80466-9

Yang Q, Sakurai T, Mori I, Yoshimura G, Nakamura M, Nakamura Y et al (2001) Prognostic significance of BRCA1 expression in Japanese sporadic breast carcinomas. Cancer 92(1):54–60. doi:10.1002/1097-0142(20010701)92:1<54::AID-CNCR1291>3.0.CO;2-8